

[Review]

Cluster Modeling of Chemisorption and Reactions on Metal Oxide Surfaces*

Xu Xin Lü Xin Wang Nan-Qin Zhang Qian-Er

(State Key Laboratory for Physical Chemistry of Solid Surfaces & Center for Theoretical Chemistry, Department of Chemistry & Institute of Physical Chemistry, Xiamen University, Xiamen 361005)

Abstract The research on the cluster modeling of chemisorption and reactions on metal oxide surfaces in our group has been reviewed. Three principles, namely, neutrality principle, stoichiometrical principle and coordination principle were proposed for building up cluster models of metal oxides. Good correlation between the topologic parameters $N_c(\beta_c)$, $N_a(\beta_a)$ and $N_d(\beta_d)$ with the stability of clusters has been shown. The problem of how the ways of embedding affect the calculated electronic properties of the substrate clusters and the adsorption properties has been investigated. Based on these, we proposed an SPC model, which is a stoichiometric cutout cluster embedded in a spherically expanded point charge surrounding with charges being self-consistently determined. We have successfully applied the SPC model to a variety of important systems, including H_2/ZnO , O/MgO , NO/MgO , N_2O/MgO , $N_2O/Li/MgO$, CO/MgO and CO/NiO .

Keywords: Cluster modeling, Oxide, Chemisorption, Surface reaction, Quantum chemistry

Metal oxides have been applied in many fields such as catalysis, corrosion, gas sensors, ceramics and high-temperature superconductivity.^[1-21] Numerous important reactions proceed over the surfaces of metal oxides; and the detailed reaction mechanisms are closely related to the nature of the oxide surfaces. While modern surface science techniques have become a powerful tool to probe the atomistic details of surface structures; theoretical modeling is now a valuable tool which complements experiment^[3-4].

A surface is of infinite size. To make computational efforts tractable, it is common to replace the surface with a small portion of substrate atoms, i. e. a cluster model^[3-15]. For a sophisticated cluster model calculation, the influence of the bulk on the cluster has to be properly taken into account. Hence in order to establish a good cluster model, one has to answer two questions: (i) how to cut out a cluster; and (ii) how to suitably account for the cluster-lattice interaction.

We reviews the activities in our group in search of the answers of these two questions for the modeling of metal oxide surfaces^[16-30]. For the first question, we have proposed three principles, namely, neutrality principle, stoichiometrical principle and coordination principle, according to which, we concluded that a

good cluster model is a neutral, stoichiometrical cut-out cluster with the minimal amount of dangling bonds^[18, 20, 24, 28]. The *ab initio* studies, taking ZnO ^[24, 28] and MgO ^[18, 20] as examples, have shown the efficiency of these principles. For the second question, our model is based on the assumption that the cluster-lattice interaction can be described by means of the Madelung potential^[16]. In contrast to the commonplace that using a point charge array to represent the surroundings of a cut-out cluster, we use spherically expanded charges and the amount of the surrounding charges is determined by a technique of self-consistency between the charge densities of the cluster atoms and those of the surroundings^[18, 19, 25, 29]. We term our model as SPC model, the main points of which are a stoichiometric cutout cluster embedded in a spherically expanded point charge surrounding with charges being self-consistently determined. We have successfully applied the SPC model to a variety of important systems, including H_2/ZnO ^[19], CO/ZnO ^[24, 30], $CO/Cu/ZnO$ ^[30], O/MgO ^[21, 26], NO/MgO ^[22-23, 27], N_2O/MgO ^[21, 26], $N_2O/Li/MgO$ ^[21], CO/MgO ^[17-18], and CO/NiO ^[16].

1 How to cut out a cluster model

An oxide in solid state can be highly ionic, like MgO , or significantly covalent, like SiO_2 . Many, like ZnO , lie somewhere in

Received: January 2, 2004; Revised: May 15, 2004. Correspondent: Xu Xin (E-mail: xinxu@xmu.edu.cn; Tel: 0592-2182219); or Wang Nan-Qin (E-mail: nxwang@xmu.edu.cn; Tel: 0592-2182658). * The Project Supported by NSFC(20021002, 29973031), the Ministry of Science and Technology of China(2001CB610506), TRAPOYT from the Ministry of Education of China and NSF of Fujian Province(2002F010)

between. Indeed, oxides differ significantly from each other in such properties as crystal structure, electronic structure. Nevertheless, there exist some basic rules that all metal oxides should obey. These are neutrality principle, stoichiometry principle and coordination principle^[18, 20, 24, 28].

We believe that neutrality principle would be the most important. Though it is not uncommon to see a charged model used to elucidate certain properties of oxide solid^[12], this kind of model degrades when being used to investigate chemisorption and surface reactions. A negatively charged model would be too active to donate electron to the adsorbate; while a positively charged one would be too eager to accept electron from adsorbate. The unrealistic electric properties of such a charged model will shift artificially the energies of its frontier orbitals, and will create spurious static interaction with adsorbate^[16, 28]. Despite that neutrality principle may be fulfilled for the whole model by choosing the opposite charge on the surrounding as opposed to that of the cluster, stoichiometry principle can never be fulfilled in a charged cluster model, and the breaking-down of stoichiometry principle will bring about some artificial DOS (density of states) of the excess atoms^[16, 28]. Thereby, we recommend using a stoichiometric cluster. In this way, neutrality requirement is reached automatically. The remainder is how to minimize the edge effect of a cluster in a given size so as to fulfill the requirement of the coordination principle.

We define N_d as the total amount of dangling bonds of a cutout cluster $(\text{MgO})_x$, and $\beta_d = N_d/2x$ as the average dangling bonds on each in-cluster atom. Similarly, we define N_a ($\beta_a = N_a/2x$) to counts up the total (average) number of the nearest neighbor missing in the cluster; We also define N_c and $\beta_c = N_c/2x$; where N_c is the summation of coordination number of each in-cluster atom and β_c denotes the average coordination number of an in-cluster atom. We anticipate a cluster with minimized $N_d(\beta_d)$ and $N_a(\beta_a)$ or maximized $N_c(\beta_c)$ is the most stable cluster. Hence the model should work best if the edge effect is the smallest^[18, 20, 24, 28].

Table 1 presents the geometries of a set of stoichiometric $(\text{MgO})_x$ ($x = 1 \sim 16$). These clusters are simple segments of the bulk. The topologic parameters $N_d(\beta_d)$, $N_a(\beta_a)$ and $N_c(\beta_c)$ of each cluster are given in Table 1^[18]. The calculated cohesive energies with *ab initio* RHF (restricted Hartree-Fock) method are also summarized in Table 1. While N_c and N_d predict that the clusters (2 b), (3 c), (4 d), (5 d), (6 c), (8 b, 8 c), (9 b), (10 c, 10 d), (12 b) and (16 a) are the most stable ones for a given x ; detailed *ab initio* calculations lead to the same conclusion. Within this set of cubic $(\text{MgO})_x$ clusters, the convergence trend on the calculated cohesive energies can be well reproduced by the trends of β_d , β_a and β_c as shown in Fig. 1. Hence it is

clear the topological parameters N_d , N_a and N_c provide an effective way to measure the relative stability of the clusters of the same size; while those of β_d , β_a and β_c measure the relative stability of clusters of different size.

Similar studies have been applied to $(\text{ZnO})_x$ ^[24, 28] and $(\text{NaCl})_x$ ^[31]. All demonstrate the effectiveness of using the topological parameters $N(\beta)$ for the guidance of cutting out clusters.

2 How to suitably account for the cluster-lattice interaction

To complete a reasonable cluster model for metal oxides, the influence of the bulk lattice has to be suitably taken into account. Neglecting the electron exchange between the cut-out cluster (C) and its surrounding (S), which is generally approximated by a point-charge array, the total energy of such an ideal system can be expressed as^[18, 25, 29]eq. (1).

$$E = \left(\Phi_C \left| \sum_{i \in C} T_i - \sum_{i \in C} \sum_{a \in C} \frac{Z_a}{r_{ia}} - \sum_{i \in C} \sum_{p \in S} \frac{Q_p}{r_{ip}} + \sum_{i > j \in C} \frac{1}{r_{ij}} \right| \Phi_C \right) + \sum_{a > b \in C} \frac{Z_a Z_b}{R_{ab}} + \sum_{a \in C} \sum_{p \in S} \frac{Z_a Q_p}{R_{ap}} + \sum_{p > q \in S} \frac{Q_p Q_q}{R_{pq}} \quad (1)$$



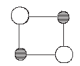
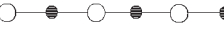
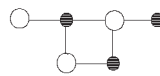
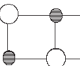

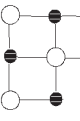
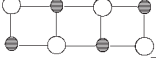




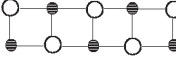





in which i, j label the electrons in cluster C, a, b label the nuclei in cluster C, while p, q label the positions of point charges in surrounding S. Φ_C is the wave function of cluster C, T_i is the electronic kinetic energy of electron i . Z_a refers to nuclear charge and r refers to distance, Q is the amount of point charge. It is common to assume the full ionicity of a metal oxide and use the nominal charges for the respective ions^[12-14]. Since most of the metal oxides are not purely ionic, but covalent to some extent in fact, the choice of full ionicity is apparently not justified.

Fig. 2 schematically shows the difference between a point charge and a real atom or ion. While a real atom processes a charge density distribution around its nucleus, the charge is concentrated on a point in a point charge model.

We argued that charge Q_p modifies the core Hamiltonian of the cluster in terms of one-electron integrals $-\sum_{i \in C} \sum_{p \in S} \frac{Q_p}{r_{ip}}$ such that different Q_p of surrounding S will deduce different Φ_C of cluster C; hence certain requirement for the consistence between the cluster and its surrounding should be met. We further showed that a better cluster modeling can be obtained if a point charge is spherically expanded so as to furnish it with a continuous distribution of charge density^[18, 25, 29].

Table 2 shows a case study, where a MgO dimer was cut out from MgO lattice and was embedded into a $998(10 \times 10 \times 10^{-2})$ point charge array. The values of the point charges Q_p 's were changed from 0.0 to ± 2.0 , in order to investigate the influence of the magnitude of the point charges on the calculated electronic properties of the embedded cluster^[25].

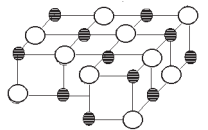


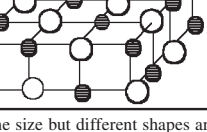
Table 1 *Ab initio* restricted Hartree-Fockⁱ calculations of (MgO)_x clusters^[18]

| <i>x</i> | Cluster ⁱ | Sym | <i>N</i> _c | β_c | <i>N</i> _d | β_d | <i>N</i> _a | β_a | <i>E</i> _c /eV ^k |
|----------|---|------------------------|-----------------------|-----------|-----------------------|-----------|-----------------------|-----------|--|
| 1a |  | <i>C</i> _{∞v} | 2 | 1.0 | 10 | 5.0 | 10 | 5.0 | -2.21 |
| 2a |  | <i>C</i> _{∞v} | 6 | 1.5 | 18 | 4.5 | 18 | 4.5 | -0.99 |
| 2b |  | <i>D</i> _{2h} | 8 | 2.0 | 16 | 4.0 | 16 | 4.0 | 0.66 |
| 3a |  | <i>C</i> _{∞v} | 10 | 1.67 | 26 | 4.33 | 26 | 4.33 | -0.12 |
| 3b |  | <i>C</i> _s | 12 | 2.0 | 24 | 4.0 | 22 | 3.67 | 0.04 |
| 3c |  | <i>C</i> _{2v} | 14 | 2.33 | 22 | 3.67 | 22 | 3.67 | 1.73 |
| 4a |  | <i>C</i> _{2v} | 20 | 2.5 | 28 | 3.5 | 27 | 3.38 | 1.64 |
| 4b |  | <i>C</i> _{2v} | 20 | 2.5 | 28 | 3.5 | 27 | 3.38 | 1.69 |
| 4c |  | <i>C</i> _{2h} | 20 | 2.5 | 28 | 3.5 | 28 | 3.5 | 2.37 |
| 4d |  | <i>T</i> _d | 24 | 3.0 | 24 | 3.0 | 24 | 3.0 | 3.11 |
| 5a |  | <i>C</i> _{1v} | 26 | 2.6 | 34 | 3.4 | 26 | 2.6 | 0.32 |
| 5b |  | <i>C</i> _{1v} | 26 | 2.6 | 34 | 3.4 | 30 | 3.0 | 1.16 |
| 5c |  | <i>C</i> ₁ | 30 | 3.0 | 30 | 3.0 | 28 | 2.8 | 2.69 |
| 5d |  | <i>C</i> _{2v} | 26 | 2.6 | 34 | 3.4 | 34 | 3.4 | 2.73 |
| 6a |  | <i>C</i> _{1v} | 30 | 2.5 | 42 | 3.5 | 26 | 2.17 | -0.61 |
| 6b |  | <i>C</i> _{2h} | 32 | 2.67 | 40 | 3.33 | 40 | 3.33 | 2.98 |
| 6c |  | <i>D</i> _{2h} | 40 | 3.33 | 32 | 2.67 | 32 | 2.67 | 3.83 |
| 7a |  | <i>C</i> _s | 46 | 3.29 | 38 | 2.71 | 34 | 2.43 | 3.06 |
| 7b |  | <i>C</i> ₁ | 46 | 3.29 | 38 | 2.71 | 36 | 2.57 | 3.49 |

Continued Table 1

| x | Cluster ¹ | Sym | N_c | β_c | N_d | β_d | N_s | β_s | E_c/eV^k |
|-----|----------------------|----------|-------|-----------|-------|-----------|-------|-----------|------------|
| 8a | | C_s | 52 | 3.25 | 44 | 2.75 | 40 | 2.5 | 3.13 |
| 8b | | C_s | 56 | 3.5 | 40 | 2.5 | 38 | 2.38 | 3.86 |
| 8c | | D_{2d} | 56 | 3.5 | 40 | 2.5 | 40 | 2.5 | 4.21 |
| 9a | | C_1 | 62 | 3.44 | 46 | 2.56 | 44 | 2.44 | 3.86 |
| 9b | | C_{4v} | 66 | 3.67 | 42 | 2.33 | 42 | 2.33 | 4.43 |
| 10a | | C_2 | 68 | 3.4 | 52 | 2.6 | 48 | 2.4 | 3.59 |
| 10b | | C_2 | 72 | 3.6 | 48 | 2.4 | 44 | 2.2 | 3.89 |
| 10c | | C_1 | 72 | 3.6 | 48 | 2.4 | 46 | 2.3 | 4.20 |
| 10d | | D_{2h} | 72 | 3.6 | 48 | 2.4 | 48 | 2.4 | 4.44 |
| 11a | | C_1 | 80 | 3.64 | 52 | 2.36 | 50 | 2.08 | 4.34 |
| 12a | | C_s | 80 | 3.64 | 52 | 2.36 | 50 | 2.08 | 4.41 |
| 12b | | D_{2d} | 88 | 3.67 | 56 | 2.33 | 56 | 2.33 | 4.59 |
| 12c | | C_{2h} | 92 | 3.83 | 52 | 2.17 | 52 | 2.17 | 4.76 |
| 13a | | C_s | 98 | 3.77 | 58 | 2.23 | 54 | 2.08 | 4.27 |
| 13b | | C_s | 98 | 3.77 | 58 | 2.23 | 54 | 2.08 | 4.28 |
| 14a | | C_2 | 108 | 3.86 | 60 | 2.14 | 56 | 2.0 | 4.44 |
| 14b | | C_1 | 108 | 3.86 | 60 | 2.14 | 58 | 2.07 | 4.64 |

Continued Table 1

| x | Cluster [†] | Sym | N_c | β_c | N_d | β_d | N_a | β_a | E_c/eV^k |
|-----|---|----------|-------|-----------|-------|-----------|-------|-----------|------------|
| 14c |  | C_1 | 108 | 3.86 | 60 | 2.14 | 58 | 2.07 | 4.68 |
| 15a |  | C_s | 118 | 3.93 | 62 | 2.07 | 60 | 2.14 | 4.75 |
| 15b |  | C_{2v} | 118 | 3.93 | 62 | 2.07 | 62 | 2.07 | 4.95 |
| 16a |  | D_{2d} | 128 | 4.0 | 64 | 2.0 | 64 | 2.0 | 5.05 |

Clusters of the same size but different shapes are labeled alphabetically.

[†] Restricted Hartree-Fock calculations with CEP-31G basis sets using Gaussian94^[92]; [‡] black dot: Mg atom; circle: O atom; ^k $E_c = E(\text{MgO}) - E[(\text{MgO})_x/x]$, where $E(\text{MgO})$ is the summation of the HF energies of atomic Mg(¹S) and O(³P); $E[(\text{MgO})_x/x]$ is the total energy of the $(\text{MgO})_x$ cluster divided by the size of the cluster, x .

For the free MgO molecule, the Mulliken charge on Mg atom is far smaller than 2.0, indicating the free MgO molecule would be quite covalent. The optimized Mg–O bond length (0.1799 nm) is far shorter than that in MgO crystal (0.2104 nm).

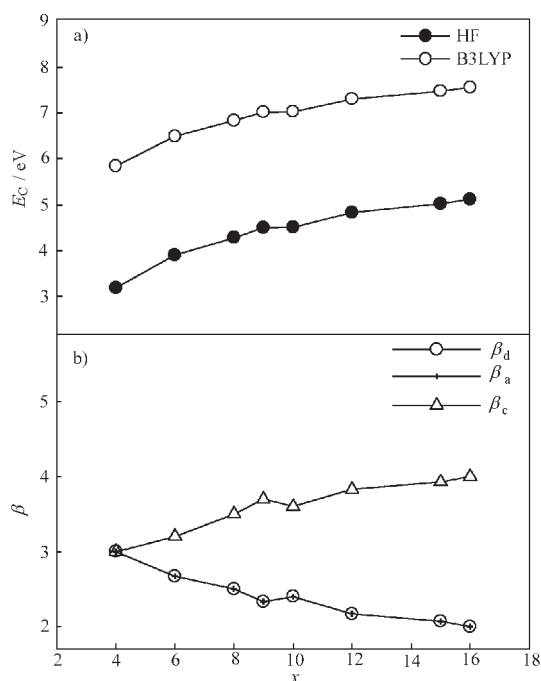


Fig. 1 Size dependence for cubic $(\text{MgO})_x$ ($x = 4, 6, 8, 9, 10, 12, 15, 16$)

(a) Convergence property of the calculated cohesive energies, E_c 's at Hartree-Fock level. calculation results with B3LYP method are also presented. (b) topological parameters β , β_a , and β_d as functions of cluster size, x ^[18]

When Q_p 's are set to be the nominal charges, (2.0, owing to the overestimation of the external field, the interaction between the cluster and the lattice point charges is non-balanced. The influence of the surrounding electric field is so strong that the optimized Mg–O distance is far longer than that in crystal. However the calculated Mulliken charges on Mg and O atoms are smaller than the nominal value 2.0.

When spherical expansion is performed on the nearest 10 point charges neighboring upon the MgO dimer, we furnish these point charges with a continuous distribution of charge density. Then when charge consistence is encountered between the embedded cluster and its surrounding, we have Q_p 's = ± 1.67 . At the same time, we have the optimized cluster geometry in accordance with the experimental lattice distance; while the calculated dipole moment of the embedded MgO dimer is also close to that of the surrounding. Hence a globe agreement is reached between the calculated properties of the embedded cluster and those of the bulk solid.

We termed our model as SPC model; the main points of

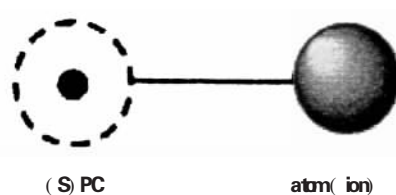


Fig. 2 Comparison between a point charge (PC), a spherically expanded point charge (SPC) and a real atom (or ion)

Table 2 *Ab initio* RHF calculations for the embedded MgO dimer^a

| Q_p | EE (a. u.) | E_{HOMO} (a. u.) | ΔG (a. u.) | Mulliken population | | | $10^{30}\mu_{\text{C}}$ (C · m) | $10^{30}\mu_{\text{S}}$ (C · m) | $R_{\text{Mg-O}}$ (nm) |
|------------|---------------|------------------------------|-----------------------|---------------------|--------|---------------------|------------------------------------|------------------------------------|---------------------------|
| | | | | Mg | O | Mg - O ^b | | | |
| ± 0.0 | -19.1066 | -0.262 | 0.211 | +0.748 | -0.748 | 1.367 | -21.21 | - | 0.2104 |
| | -19.6459 | -0.284 | 0.227 | +1.021 | -1.021 | 1.531 | -28.82 | | 0.1799* |
| ± 2.0 | -21.9178 | -0.440 | 0.472 | +1.784 | -1.784 | 0.316 | -65.84 | 67.41 | 0.2104 |
| | -22.2232 | -0.427 | 0.444 | +1.820 | -1.820 | 0.341 | -90.76 | | 0.2926* |
| ± 1.67 | -21.3916 | -0.392 | 0.363 | +1.668 | -1.668 | 0.419 | -62.78 | 62.81 | 0.2104 |
| (10SPC) | -21.3954 | -0.393 | 0.365 | +1.667 | -1.667 | 0.421 | -62.38 | | 0.2088* |

^a Mg: $3s^2$, O: $2s^22p^4$; Basis sets: CEP-31G⁽³²⁾ (Calculated with Hondo8⁽³³⁾ and Gaussian94⁽³²⁾); ^b Hondo8 bond order⁽³³⁾ (EE: electronic energy; ΔG , HOMO, LUMO gap;

* Results under optimized geometry)⁽²⁵⁾

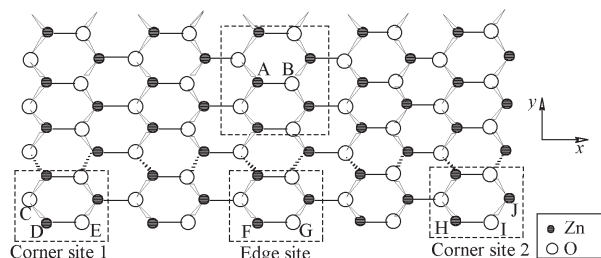
which are a stoichiometric cutout cluster embedded in a spherically expanded point charge surrounding with charges being self-consistently determined. Case studies in our group^[16-30] and other groups^[31, 35-37] of chemisorption on the metal oxides of different degree of ionicity demonstrated the efficiency of the SPC model.

3 Some applications of the SPC model

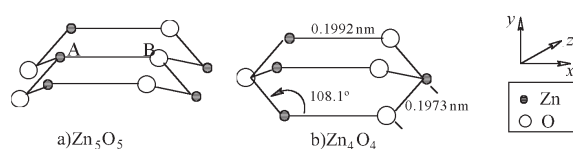
3.1 Heterolytic adsorption of H₂ on ZnO surface⁽¹⁹⁾

The adsorption of H₂ on ZnO has been of interest for several decades due to its close relationship with some important industrial processes, e. g. hydrogenation of olefin, methanol synthesis from syngas, and water-gas shift reaction. Plenty of experimental evidences showed that ZnO works to provide sites for the chemisorption of H₂^[38-41]. The experimental observation thereby implies that no regular Zn_{3C}-O_{3C} ion-pairs of these surfaces should be responsible for the dissociative chemisorption of H₂, and that the most possibly active sites should be those defective surface sites, such as Zn_{2C}-O_{3C}, Zn_{3C}-O_{2C} and Zn_{2C}-O_{2C}, presenting at the edge and corner sites of ZnO surfaces.

Fig. 3 shows the ideal surface, where the A-B site is a regular Zn_{3C}-O_{3C} ion-pair represented by a (ZnO)₅ cluster (Fig. 4). A (ZnO)₄ cluster (Fig. 4) is used to model the Zn_{2C}-O_{3C} (D-C) or the Zn_{2C}-O_{2C} (D-E) on the corner site 1; the Zn_{2C}-O_{2C} (F-G) at the edge site; and the Zn_{2C}-O_{2C} (H-I) or the Zn_{3C}-O_{2C} (J-I) on the corner site 2 (Fig. 3). Here (ZnO)₄ and (ZnO)₅ are the stoichiometric clusters having the least amount of dangling bonds in the

**Fig. 3** Structure of the ZnO wurtzite crystal lattice

top-view of the ZnO(1010) surface. The active sites for H₂ chemisorption are labeled alphabetically. ⁽¹⁹⁾

**Fig. 4** Zn₅O₅ and Zn₄O₄ clusters as models of the ZnO (1010) surface⁽¹⁹⁾

metric clusters having the least amount of dangling bonds in the given size. Fig. 3 consists of a six-layer model of a total of 630 lattice atoms, within which the rest of the atoms are replaced by spherical charges being determined by the charge-consistency technique.

Table 3 summarizes the calculated geometries, heats and frequencies for H₂/ZnO chemisorption system at the MP2 level. In accordance with the experimental findings, we predicted that the heterolytic adsorption of H₂ on ZnO (1010) surface is site-dependent, taking place only on those Zn-O ion-pairs with low coordination numbers, such as Zn_{2C}-O_{3C}, Zn_{3C}-O_{2C} and Zn_{2C}-O_{2C}, rather than on the perfect ion pair, Zn_{3C}-O_{3C}. We also find that the effect of the crystal potential is significant. The results from the bared cluster model calculations could only be regarded as qualitative. The calculated adsorption heats with the bare Zn₄O₄ cluster models are either too low (12.6 ~ 33.5 kJ · mol⁻¹) or too high (272.0 ~ 364.8 kJ · mol⁻¹) as compared with the experimental value (~125.5 kJ · mol⁻¹); while the calculated adsorption heats with the SPC embedded cluster models are in good agreement with the experimental values (SPC model yields adsorption energies of 125.5 kJ · mol⁻¹ at edge site and 131.4 kJ · mol⁻¹ at the corner 2 site). The predicted Zn-H and O-H stretching frequencies are in reasonable accordance with those of the IR spectra (Table 3). The frequencies of X-H (X = Zn, O) show dependence on the coordination number of the respective X ion, i. e. the Zn_{2C}-H and O_{2C}-H stretching frequencies are much higher than those of the Zn_{3C}-H and O_{3C}-H vibrations, respectively. It is also found that the lower coordina-

Table 3 Calculated geometries, heats^a and frequencies for H₂/ZnO chemisorption system at MP2 level

| Cluster Model ^b (active sites) | R_{OH}/nm | $\angle \text{HOM} (^{\circ})$ | R_{MH}/nm | $\angle \text{HMO} (^{\circ})$ | $\Delta E/\text{kJ} \cdot \text{mol}^{-1}$ | ν_e/cm^{-1} | |
|--|--------------------|--------------------------------|--------------------|--------------------------------|--|------------------------|--------------------|
| | | | | | | Zn - H | O - H |
| Zn ₃ O ₃ | | | | | | | |
| Zn _{3c} -O _{3c} (A-B) | Bared ^d | 0.0965 | 95.5 | 0.1774 | 81.2 | -115.1 | |
| | Embedded | 0.0985 | | 0.1735 | | -97.1 | 1341, 3531 |
| Zn ₄ O ₄ | | | | | | | |
| Zn _{2c} -O _{3c} (D-C) | Bared ^d | 0.0961 | 93.8 | 0.1642 | 93.5 | 12.6 | |
| | Corner 1 | 0.0980 | | 0.1627 | | 161.1 | 1652, 3705 |
| Zn _{3c} -O _{2c} (J-I) | Bared ^d | 0.0954 | 120.6 | 0.1710 | 93.8 | 23.4 | |
| | Corner 2 | 0.0977 | | 0.1664 | | 149.0 | 1570, 3778 |
| Zn _{2c} -O _{2c} (F-G) | Bared ^d | 0.0952 | 121.1 | 0.1617 | 124.0 | 272.0 | |
| | Edge | 0.0971 | | 0.1589 | | 125.5 | 1805, 3851 |
| Zn _{2c} -O _{2c} (D-E) | Corner 1 | 0.0951 | | 0.1644 | | 193.3 | 1621, 4092 |
| Zn _{2c} -O _{2c} (H-I) | Corner 2 | 0.0954 | | 0.1589 | | 131.4 | 1850, 4124 |
| Exptl. | | | | | | ~125.5 ^e | 1485, 3385 |
| | | | | | | -1753 ^d | -3495 ^d |

^a Positive value of ΔE means exothermicity; ^bThe two letters in parentheses followed each cluster denote the active Zn and O ions, respectively, as those labeled in Fig. 3; ^c Ref. [42-43]; ^d Ref. [44]; ^e geometry optimized at Hartree-Fock level

tion number X ion possesses, the shorter the H - X bond length is.

3.2 Adsorption and decomposition of NO on Magnesium oxide^[23]

The mechanistic understanding of catalytical decomposition and reduction of NO_x is of great importance in pollution control. For NO decomposition on metal oxide surfaces, the mechanism is not well-known, despite the fact that there have been several experimental efforts on this topic, from the earlier systematic work of Winter^[44-45] to the recent work of Acke *et al.*^[46]. Prior to our work, no detailed theoretical work has been done on the NO/MgO system. We have considered the adsorptions of NO and (NO)₂ at the terrace, step, corner and island sites of MgO(100) surface. We aimed to address (a) how NO adsorbs; (b) what kinds of surface species work as intermediates in NO decomposition and (c) by which way the intermediates are produced^[23].

Fig. 5 presents the cluster models used in the studies. We found NO adsorbed on the low-coordinate sites in a chain modes (Fig. 6). The binding energy follows the order that Mg_{3c}-O_{3c} (34.6) > Mg_{3c}-O_{4c} (15.1) > Mg_{4c}-O_{3c} (12.0) > Mg_{4c}-O_{4c}

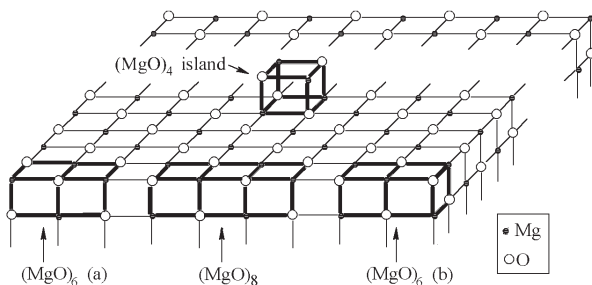


Fig. 5 The low-coordinate sites on a (10 × 10 × 10) microcrystal as well as the corresponding embedded cluster models^[23]

(23.0 kJ·mol⁻¹). We found a large charge transfer (~0.6 a.u.) from lattice oxygen to the adsorbed NO so that the adsorbate NO combined with the lattice O²⁻ can be regarded as a (NO₂)²⁻ surface species. This result is supported by the electron spin resonance experiments^[48-49].

Our calculations revealed that a second NO can be adsorbed on top of (NO₂)²⁻, leading to the formation of N₂O₃²⁻ surface species. Fig. 7 depicts two configurations of N₂O₃²⁻, whose calculated vibrational frequencies were compared with IR spectra of NO/MgO adsorption system^[50] and those of solid Na₂N₂O₃, Na₂N₂O₂ and NaNO₂^[51] (Table 4). Data in Table 4 strongly support our conclusion about the formation of N₂O₃²⁻ surface species.

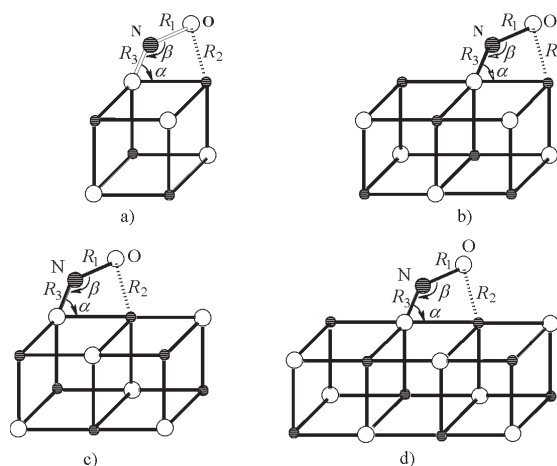


Fig. 6 Chain mode of monomeric NO adsorbed on the Mg_{Xc}-O_{Yc} (X, Y = 3, 4) pair sites modeled by the embedded (MgO)_n (n = 4, 6, 8) clusters. The black dot is Mg, and the white circle is O. The surrounding of (MgO)_n is not shown.

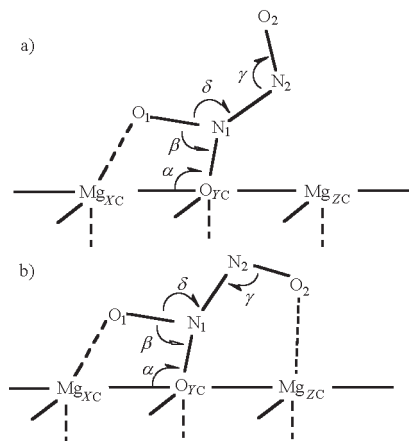


Fig. 7 Two configurations of $\text{N}_2\text{O}_3^{2-}$ surface species

a) cis- $\text{N}_2\text{O}_3^{2-}$; b) trans- $\text{N}_2\text{O}_3^{2-}$ ^[23]

Based on the geometry and energetics of $\text{N}_2\text{O}_3^{2-}$ surface species, an NO decomposition mechanism can easily be conjectured: while the cis- $\text{N}_2\text{O}_3^{2-}$ would lead to the formation of $\text{O} + \text{N}_2\text{O}$; the trans- $\text{N}_2\text{O}_3^{2-}$ would lead to the formation of $2\text{O} + \text{N}_2$.

3.3 N_2O decomposition on MgO and Li/MgO catalysts^[21]

The decomposition of N_2O on metal oxides is of industrial importance. Practically, N_2O is always used as an oxidant in a lot of catalyzed oxidative processes, such as oxidative coupling of methane (OCM), oxidative dehydrogenation of alkanes^[52-56]. N_2O was suggested to provide adsorbed oxygen species on metal oxide catalysts and hence leads to more specific oxidative selectivity than O_2 does^[56].

We have performed SPC model study on the decomposition of N_2O on MgO and Li/MgO catalysts (Fig. 5). We found on MgO(100) terrace N_2O is adsorbed on top of the O_{3c} anions with a binding energy of $105.9 \text{ kJ} \cdot \text{mol}^{-1}$. On the corners or steps, the preferred mode is for atomic oxygen to bridge over the low-coordinated $\text{O}_{xc}\text{-Mg}_{yc}$ ($X, Y=3, 4$) ion pairs. The binding energies are between 190.0 and $253.6 \text{ kJ} \cdot \text{mol}^{-1}$. We predicted the adsorption of atomic oxygen at the corners and steps leads to the formation of a peroxide ion with the $\text{O}_{ad} - \text{O}_{xc}$ stretching fre-

quencies in the range $819 \sim 857 \text{ cm}^{-1}$.

Fig. 8 shows the geometries of the transition states of N_2O decomposition over (a) $\text{O}_{3c}\text{-Mg}_{3c}$, (b) $\text{O}_{3c}\text{-Mg}_{4c}$, (c) $\text{O}_{4c}\text{-Mg}_{3c}$, and (d) $\text{O}_{4c}\text{-Mg}_{4c}$ pair sites modeled by the embedded $(\text{MgO})_n$ clusters. We found that the activity of the $\text{O}_{xc}\text{-Mg}_{yc}$ ($X, Y=3, 4$) ion pairs toward N_2O decomposition follows the order that $\text{O}_{3c}\text{-Mg}_{3c} > \text{O}_{4c}\text{-Mg}_{3c} > \text{O}_{3c}\text{-Mg}_{4c} > \text{O}_{4c}\text{-Mg}_{4c}$. The corresponding barrier heights (E_a) and reaction heats ($-\Delta E$) are (85.8, 117.2), (101.3, 58.2), (118.4, 39.3) and (120.9, 22.6) in $\text{kJ} \cdot \text{mol}^{-1}$. The O_{4c} site is the least active. $(\text{MgO})_5$ (5a in Table 1) model predicted an activation barrier of 175.7 and an endothermicity of $80.3 \text{ kJ} \cdot \text{mol}^{-1}$.

Fig. 9 shows the geometry of the transition state of N_2O decomposition on the $[\text{Li}^+\text{O}^-]$ center. When the MgO catalyst is doped with Li, the so-called $[\text{Li}^+\text{O}^-]$ centers are found to be ac-

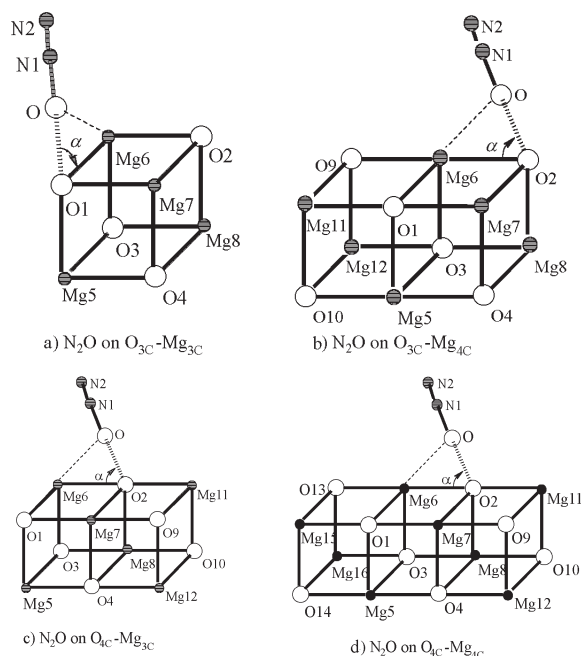


Fig. 8 Geometries of the transition states of N_2O decomposition

(a) $\text{O}_{3c}\text{-Mg}_{3c}$, (b) $\text{O}_{3c}\text{-Mg}_{4c}$, (c) $\text{O}_{4c}\text{-Mg}_{3c}$, and (d) $\text{O}_{4c}\text{-Mg}_{4c}$ pair sites modeled by the embedded $(\text{MgO})_n$ clusters^[21]

Table 4 Calculated IR frequencies of $\text{N}_2\text{O}_3^{2-}$ surface complexes as well as experimental spectra of NO/MgO chemisorption system, and solid $\text{Na}_2\text{N}_2\text{O}_3$, $\text{Na}_2\text{N}_2\text{O}_2$ and NaNO_2

| | | | ν_1/cm^{-1} | ν_2/cm^{-1} | ν_3/cm^{-1} | ν_4/cm^{-1} |
|---|-----------------------|-------|------------------------|------------------------|------------------------|------------------------|
| NO/MgO system | Present work | a | 1472 | 1415 | 1097 | 917 |
| | | b | 1534 | 1269 | 1110 | |
| | Expt. ^[50] | 77 K | 1450 ~ 1350 | 1313 | 1250 ~ 1100 | 893 |
| | | R. T. | 1500 ~ 1350 | 1250 | 1100 | |
| N_2O_3 in $\text{Na}_2\text{N}_2\text{O}_3$ | Expt. ^[51] | | 1400 | 1280 | 1120 | 975 |
| N_2O_2 in $\text{Na}_2\text{N}_2\text{O}_2$ | Expt. ^[51] | | 1313 | 1047 | | |
| NO_2^- in NaNO_2 | Expt. ^[51] | | 1337 | 1270 | 829 | |

a) ν_1 : N-N stretch; ν_2 : N-O sym. stretch. b) ν_1 : N-O bonds sym. stretch; ν_2 : N-O bonds antisym. stretch; ν_3 : ONO bend; ν_4 : N-O stretch

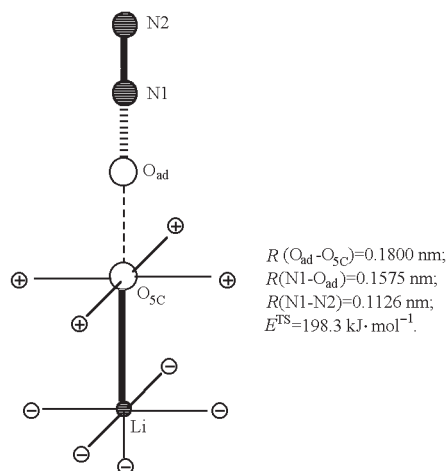


Fig. 9 Geometry of the transition state of N₂O decomposition on the [Li⁺O⁻] center^[21]

tive for decomposing N₂O. LiMg₄O₅ model predicted (E_a , $-\Delta E$) are (149.0, 35.6 kJ·mol⁻¹). This accounts for the experimentally observed promotion effect of Li-doping on the catalytic reaction^[55-56]. The decomposition of N₂O on the active [Li⁺O⁻] center leads to the formation of the superoxide anion, which would be the reason for the high C₂ selectivity in the OCM reaction.

4 Concluding remarks

In the frame work of an embedded cluster model, a bulk solid may be regarded as a sum of two fragments: one is a cutout cluster explicitly treated with quantum mechanics; the other is the surrounding of the cutout cluster. Accordingly, in order to establish a reasonable embedded cluster model, one has to answer two questions: (i) how to cut out a cluster; and (ii) how to suitably account for the cluster-lattice interaction. For the first question, we have proposed three principles, namely, neutrality principle, stoichiometrical principle and coordination principle, according to which a neutral, stoichiometrical cut-out cluster with the minimal amount of dangling bonds is preferred. We have shown the good correlation between the topologic parameters N_c (β_c), N_a (β_a), and N_d (β_d) with the stability of clusters. We believe that these topologic parameters provide meaningful criteria to cut out a better cluster model without paying for the high cost of detailed preliminary calculations. For the second question, we have demonstrated how the calculated electronic properties of the substrate clusters and the adsorption properties vary with the ways to describe the surrounding. We argued that it is most important to reach charge density consistency so that the bulk surrounding can be best described with an array of spherically expanded point charges. It is shown that an SPC model, i. e. a stoichiometric cutout cluster with the least dangling bonds embedded in a sym-

metric PC array, and a spherically expanded point charge surrounding with charges being self-consistently determined, provides an efficient way to describe the electronic properties of the bulk and solid and surfaces, as well as the chemisorption and reactions on the metal oxide surfaces.

References

- 1 Kung, H. H. Transition metal oxides: surface chemistry and catalysis. Amsterdam: Elsevier, 1989
- 2 Freund, H. -J. ; Umbach, E. (eds.). Adsorption on ordered surfaces of ionic solids and thin films. Berlin: Springer, 1994
- 3 Sauer, J. ; Ugliengo, P. ; Garrone, E. *Chem. Rev.*, **1994**, *94*: 2095
- 4 Colbourn, E. A. *Surf. Sci. Rep.*, **1992**, *15*: 281
- 5 Jug, K. ; Geudtner, G. ; Bredow, T. *J. Mol. Catal.*, **1993**, *82*: 171
- 6 Sauer, J. *Chem. Rev.*, **1989**, *89*: 199
- 7 Pisani, C. ; Cora, F. ; Nada, R. ; Orlando, R. *Comput. Phys. Commun.*, **1994**, *82*: 139
- 8 Whitten, J. L. *Chem. Phys.*, **1993**, *177*: 387
- 9 Lopez-Moraza, S. ; Pascual, J. L. ; Barandiaran, Z. *J. Chem. Phys.*, **1995**, *103*: 2117
- 10 Mejias, J. A. ; Fernandez, J. F. *J. Chem. Phys.*, **1995**, *102*: 327
- 11 Vail, J. M. ; Rao, B. K. *Int. J. Quantum Chem.*, **1995**, *53*: 67
- 12 Pacchioni, G. ; Cogliandro, G. ; Bagus, P. S. *Int. J. Quantum Chem.*, **1992**, *42*: 1115
- 13 Pacchioni, G. ; Minerva, T. *Surf. Sci.*, **1992**, *275*: 450
- 14 Nygren, M. A. ; Pettersson, L. G. ; Barandiaran, M. Z. ; Seijo, L. *J. Chem. Phys.*, **1994**, *100*: 2010
- 15 Mejias, J. A. ; Marquez, A. M. ; Fernandez-Garcia, J. M. ; Ricart, J. M. ; Sousa, C. ; Illas, F. *Surf. Sci.*, **1995**, *327*: 59
- 16 Xu, X. ; Lu, X. ; Wang, N. Q. ; Zhang, Q. E. *Chem. Phys. Lett.*, **1995**, *235*: 541
- 17 Lu, X. ; Xu, X. ; Wang, N. Q. ; Zhang, Q. E. *J. Phys. Chem.*, **2000**, *B104*: 10024
- 18 Xu, X. ; Nakatsuji, H. ; Lu, X. ; Ehara, M. ; Cai, Y. ; Wang, N. Q. ; Zhang, Q. E. *Theor. Chem. Acc.*, **1999**, *102*: 170
- 19 Lu, X. ; Xu, X. ; Wang, N. Q. ; Zhang, Q. E. ; Ehara, M. ; Nakatsuji, H. *J. Phys. Chem.*, **1999**, *B103*: 2689
- 20 Lu, X. ; Xu, X. ; Wang, N. Q. ; Zhang, Q. E. *Int. J. Quantum Chem.*, **1999**, *73*: 377
- 21 Lu, X. ; Xu, X. ; Wang, N. Q. ; Zhang, Q. E. *J. Phys. Chem. B*, **1999**, *103*: 3373
- 22 Lu, X. ; Xu, X. ; Wang, N. Q. ; Zhang, Q. E. *Chem. Phys. Lett.*, **1999**, *300*: 109
- 23 Lu, X. ; Xu, X. ; Wang, N. Q. ; Zhang, Q. E. *J. Phys. Chem.*, **1999**, *B103*: 5657
- 24 Lu, X. ; Xu, X. ; Wang, N. Q. ; Zhang, Q. E. *Chem. J. Chin. Univ.*, **1998**, *19*: 783 [吕鑫,徐昕,王南钦,张乾二. 高等学校化学学报 (*Gaodeng Xuexiao Huaxue Xuebao*), **1998**, *19*: 783]
- 25 Xu, X. ; Nakatsuji, H. ; Ehara, M. ; Lu, X. ; Wang, N. Q. ; Zhang, Q. E. *Science in China*, **1998**, *B41*: 113

- 26 Lu, X.; Xu, X.; Wang, N. Q.; Zhang, Q. E. *Chin. Chem. Lett.*, **1998**, **9**: 583
- 27 Lu, X.; Xu, X.; Wang, N. Q.; Zhang, Q. E. *Chem. Res. Chin Univ.*, **1998**, **14**(2): 215
- 28 Lu, X.; Xu, X.; Wang, N. Q.; Zhang, Q. E.; Ehara, M.; Nakatsuji, H. *Chem. Phys. Lett.*, **1998**, **291**: 445
- 29 Xu, X.; Nakatsuji, H.; Ehara, M.; Lu, X.; Wang, N. Q.; Zhang, Q. E. *Chem. Phys. Lett.*, **1998**, **292**: 282
- 30 Lu, X.; Xu, X.; Wang, N. Q.; Zhang, Q. E. *Acta Phys.-Chim. Sini.*, **1997**, **13**(11): 1005 [吕鑫,徐昕,王南钦,张乾二. *物理化学学报 (Wuli Huaxue Xuebao)*, **1997**, **13**(11): 1005]
- 31 Lai, J. F.; Lu, X.; Zheng, L. S. *Phys. Chem. Comm.*, **2002**: 82
- 32 Frisch, M. J.; Trucks, G. W.; Schlegel, H. B.; et al. *Gaussian 94*. Revision D. 2. Pittsburgh, PA: Gaussian, Inc, 1995
- 33 Dupuis, M.; Farazdel, A.; King, H. F. et al. *Hondo 8 from MOTECC-91*. NY 12401 USA: IBM Corporation, Center for Scientific & Engineering Computations, 1995
- 34 Taylor, H. S.; Strother, C. O. *J. Am. Chem. Soc.*, **1934**, **56**: 589
- 35 Li, J. Q.; Xu, Y. J.; Zhang, Y. F. *Solid State Comm.*, **2003**, **126**: 107
- 36 Xu, Y. J.; Li, J. Q.; Zhang, Y. F.; Chen, W. K. *Surf. Sci.*, **2002**, **525**: 13
- 37 Xu, Y. J.; Li, J. Q.; Zhang, Y. F. *Surf. Rev. Lett.*, **2003**, **10**: 691
- 38 Eischens, R. P.; Pliskin, W. A.; Low, M. J. D. *J. Catal.*, **1962**, **1**: 180
- 39 Dent, A. L.; Kokes, R. J. *J. Phys. Chem.*, **1969**, **73**: 3781
- 40 Baranski, A.; Cvetanovic, R. J. *J. Phys. Chem.*, **1971**, **75**: 208
- 41 Bowker, M.; Houghton, H.; Waugh, K. C. *J. Chem. Soc., Faraday Trans. (1)*, **1981**, **77**: 3023
- 42 Waugh, K. C. *Catalysis Today*, **1992**, **15**: 51
- 43 Ghiotti, G.; Chiorino, A.; Bocuzzi, F. *Surf. Sci.*, **1993**, **287**: 228
- 44 Winter, E. R. S. *J. Catal.*, **1971**, **22**: 158
- 45 Winter, E. R. S. *J. Catal.*, **1974**, **34**: 440
- 46 Acke, F.; Panas, I.; Stromberg, D. *J. Phys. Chem. B*, **1997**, **10**: 6484
- 47 Lunsford, J. K. *J. Chem. Phys.*, **1967**, **46**: 4347
- 48 Zhang, G.; Tanaka, T.; Yamaguchi, T.; Hattori, H.; Tanabe, K. *J. Phys. Chem.*, **1990**, **94**: 506
- 49 Platero, E. E.; Spoto, G.; Zecchina, A. *J. Chem. Soc., Faraday Trans. (1)*, **1985**, **81**: 1283
- 50 Laane, J.; Ohlsen, J. R. *Prog. Inorg. Chem.*, **1980**, **27**: 465 and references therein
- 51 Winter, E. R. S. *J. Catal.*, **1970**, **19**: 32
- 52 Ward, M. B.; Lin, M. J.; Lunsford, J. H. *J. Catal.*, **1977**, **50**: 306
- 53 Ito, T.; Wang, J.-X.; Lin, C. H.; Lunsford, J. H. *J. Am. Chem. Soc.*, **1985**, **107**: 5062
- 54 Nakamura, M.; Mitsuhashi, H.; Takezawa, N. *J. Catal.*, **1992**, **138**: 686
- 55 Yamamoto, H.; Chu, H. Y.; Xu, M.; Shi, C.; Lunsford, J. H. *J. Catal.*, **1993**, **142**: 325
- 56 Hutchings, G. J.; Scurrel, M. S.; Woodhouse, J. R. *Chem. Soc. Rev.*, **1989**, **18**: 251

金属氧化物表面化学吸附和反应的量子化学簇模型方法研究

徐昕 吕鑫 王南钦 张乾二

(厦门大学化学系, 固体表面物理化学国家重点实验室, 理论化学研究中心, 物理化学研究所, 厦门 361005)

摘要 综述了本研究小组利用量子化学簇模型方法研究金属氧化物表面化学吸附和反应的工作. 提出了选簇的三个原则, 即电中性原则、化学配比原则和配位原则. 发现在符合前两个原则的基础上, 一个具有最饱和配位、或最少悬空键的簇往往是一个用于化学吸附研究的好的簇模型. 与此同时, 探讨了如何恰当地考虑大块固体本底的长程影响, 提出了用球电荷模拟簇模型的环境、环境与簇体进行电荷自洽的 SPC 簇模型方法. 利用该模型研究了一系列具有催化背景的重要体系, 包括 H_2/ZnO 、 O/MgO 、 NO/MgO 、 N_2O/MgO 、 $N_2O/Li/MgO$ 、 CO/MgO 、 CO/NiO 等.

关键词: 簇模型方法, 氧化物, 化学吸附, 表面反应, 量子化学

中图分类号: O641